

# Mechanical properties of as-cast and extruded Mg-4Zn and Mg-4Zn-0.4Ca alloys

M. Hradilová\*, D. Vojtěch

*Institute of Chemical Technology Prague, Department of Metals and Corrosion Engineering,  
Technická 5, 166 28 Prague 6, Czech Republic*

Received 20 October 2013, received in revised form 29 August 2014, accepted 17 September 2014

## Abstract

This work studied the effect of extrusion and alloying with 4 wt.% of Zn and 0.4 wt.% of Ca on the structure and mechanical properties of magnesium. Light, scanning electron microscopy, X-ray diffraction, hardness, compressive and tensile tests were used for this purpose. The addition of zinc led to the formation of MgZn and further alloying with calcium changed the nature of the secondary phase to  $\text{Ca}_2\text{Mg}_6\text{Zn}_3$ . The process of extrusion resulted in significant structural refinement, which was the most pronounced for the Mg-4Zn-0.4Ca alloy. In this alloy the average grain size was 6  $\mu\text{m}$ . The extrusion improved all the measured characteristics and the most pronounced improvement was observed in the case of tensile yield strength. The presence of calcium improved the positive effect of zinc on the mechanical properties of magnesium. Differences in the mechanical behaviour of magnesium and its alloys were discussed in relation to structural variations resulting in different strengthening effects.

**Key words:** magnesium alloys, microstructure, extrusion, mechanical properties

## 1. Introduction

Present demand of numerous producers in various areas for reducing the weight of construction parts significantly increases the interest in magnesium and its alloys. Magnesium is namely regarded to become the most lightweight construction material in future. Magnesium with density of  $1.7 \text{ g cm}^{-3}$  is nearly five times lighter than steel and even lighter than aluminium (approximately 30 % less) [1–3]. It is the eighth most abundant element in the earth's crust and its reserves are almost unlimited due to the presence in sea water.

Recently, magnesium alloys have been mainly used in the form of castings. However, the as-cast alloys cannot achieve desired mechanical properties (strength, ductility, toughness, hardness) only via suitable alloying or modifying the conditions of solidification [4–6]. To improve the strength characteristics, the appropriate processing methods like extrusion, forging, rolling are widely applied [2, 3]. On the other hand, workability of magnesium and its alloys at ambient temperatures is poor due to an inadequate number of slip systems in its hexagonal crystal structure. This

limitation can only be overcome at higher forming temperatures [7]. In some magnesium alloys, higher temperatures of forming may initiate the formation of fine precipitates [9, 10], which can however contribute to obtain a finer structure [11] and to stabilize it. This also extends possible applications of such alloys as well as the applications at elevated temperatures [10]. Additionally, high-temperature stability can be enhanced via alloying with rare-earth elements (RE), which form thermally stable Mg-RE precipitates representing effective obstacles for dislocation slip at elevated temperatures [8, 9]. However, the high cost of rare-earth elements limits the extensive use of such alloys. In spite of that, alkaline-earth metals, such as Ca or Sr, can be alternative alloying elements, which may induce formation of intermetallic phases with high congruent melting points leading to an increase in the mechanical properties at elevated temperatures [10–12].

Zinc is – next to aluminium – one of the most used alloying elements with the advantages, such as increase of the strength of Mg alloys, improvement of the castability [8, 13–15]. Besides, the addition of zinc

\*Corresponding author: tel.: +420 2 20444055; fax: +420 2 20444400; e-mail address: [hradilom@vscht.cz](mailto:hradilom@vscht.cz)

Table 1. The chemical compositions of the investigated alloys (in wt.%)

	Zn	Ca	Al	Si	Fe	Mn	Ni	Mg
Mg-4Zn	3.69	<0.04	<0.02	<0.03	<0.01	<0.02	<0.01	bal.
Mg-4Zn-0.4Ca	3.76	0.41	<0.02	<0.03	<0.02	<0.01	<0.01	bal.

leads to enhancement of corrosion resistance. Previous studies [16–19] showed that optimum amount of zinc with appropriate mechanical and corrosion properties is about 4 wt.%. In addition, zinc and calcium can be well metabolized by human body [14], which makes them more attractive for their using as effective alloying element of magnesium. From the wide spectrum of possible thermo-mechanical processes, the extrusion was selected as one of the most used large-scale manufacturing methods, which enables to convert a cast billet to a finished wrought product [7]. Overall, using of low cost alloying elements such as Zn and Ca in combination with the extrusion may be cost-effective way which would allow to prepare magnesium alloys with appropriate properties. Therefore, the aim of this study is to characterize how the structure and mechanical properties of magnesium are changed by addition of appropriate amount of zinc and calcium and subsequent application of hot extrusion. The other aim is to verify if such a small addition of calcium may more significantly influence mechanical properties of Mg-4Zn alloy.

## 2. Experimental details

Pure magnesium (99.99 %) and two alloys with nominal chemical compositions of Mg-4Zn and Mg-4Zn-0.4Ca (wt.%) were studied in this work. The magnesium alloys were prepared by induction melting (Balzers VSG-02 vacuum furnace) of pure Mg (99.99 %), Zn (99.96 %) and an Mg-10Ca (wt.%) master alloy under argon atmosphere in a graphite crucible followed by casting into a steel mould to prepare cylindrical ingots of 20 mm diameter and 100 mm length. The chemical compositions of both alloys were verified by X-ray fluorescence analysis (XRF) summarized in Table 1.

The prepared ingots were heat-treated at 340 °C for 24 h before hot extrusion. The hot extrusion was realized at a temperature of 350 °C, an extrusion ratio of 10:1 and a deformation rate of 5 mm min<sup>-1</sup>. Before extrusion, the materials were held at the processing temperature for 10 min.

The microstructures of as-cast (denoted as C) and extruded (denoted as E) alloys were studied by light microscopy (LM; Olympus PME3) and scanning electron microscopy (SEM; Tescan Vega3 LMU) equipped with energy dispersive spectrometry (EDS, Oxford In-

struments Inca 350). Preparation of samples consisted of mechanical grinding, polishing and final etching with an acetic-picric solution (4.2 g picric acid, 10 ml acetic acid, 70 ml ethanol, 10 ml water). The microstructures were examined on sections parallel to the extrusion direction (ED). The average grain size was determined via image software LUCIE on the basis of the equivalent diameter. For this purpose more than 200 grains were analysed.

Mechanical properties were examined by Vickers hardness with a load of 5 kg, compressive and tensile tests. For compressive tests, cylindrical samples of 9 mm height and 6 mm diameter were used. Tensile samples had a length and diameter of 25 and 3 mm, respectively. Compressive and tensile tests were conducted on a LabTest 5.250SP1-VM universal loading machine with a strain rate of 0.001 s<sup>-1</sup> and at the room temperature (RT). In all cases the loading direction was parallel to the extrusion direction, as well as to the longitudinal axis of the as-cast ingots. In addition, the tensile and compressive tests were performed two or four times and standard deviations were calculated. The hardness measurements were done usually ten times and the standard deviation was estimated.

Crystallographic textures were determined in the centre-plane of the samples treated via extrusion. Texture measurements were conducted in reflection geometry on PANalytical X-ray diffractometer X'Pert PRO equipped with the texture cradle (ATC-3) using Co K $\alpha$  radiation at 43 kV and 20 mA. The incomplete pole figures of diffraction 100, 002, 101 and 011, which corresponds to 10 $\bar{1}$ 0, 0002, 10 $\bar{1}$ 1, 01 $\bar{1}$ 1 in hcp, were used for calculation of orientation distribution function (ODF). The samples were tilted from 0° up to 70°, azimuthal rotations were done from 0° up to 350°, both with the step of 10°. Afterwards, the complete pole figures of (0002) direction were calculated from ODF with the use of the X'Pert Texture software. In addition, the defocusing and background corrections were made.

## 3. Results and discussion

### 3.1. Microstructure

Figure 1 shows the microstructure of pure magnesium after casting and hot extrusion at 350 °C. The as-cast magnesium contains large elongated grains of

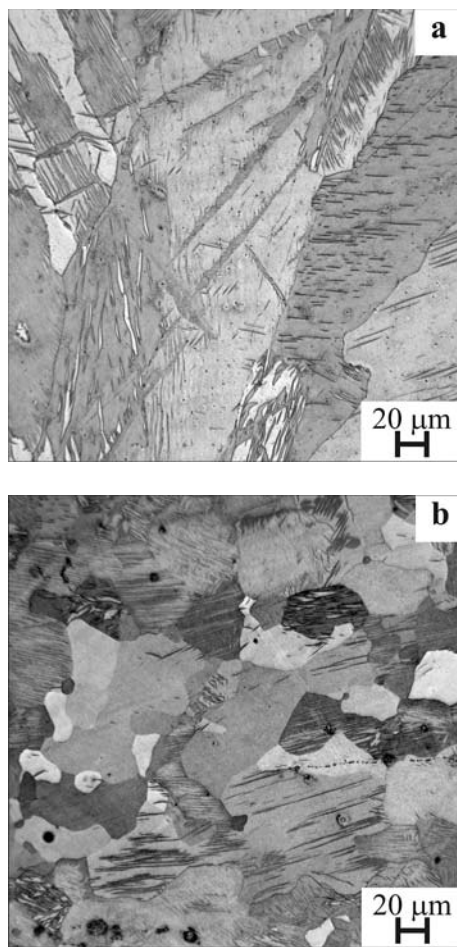


Fig. 1. Microstructure of pure magnesium in the as-cast (a) and extruded (b) states. (The horizontal direction of figures of extruded material represents the extrusion direction.)

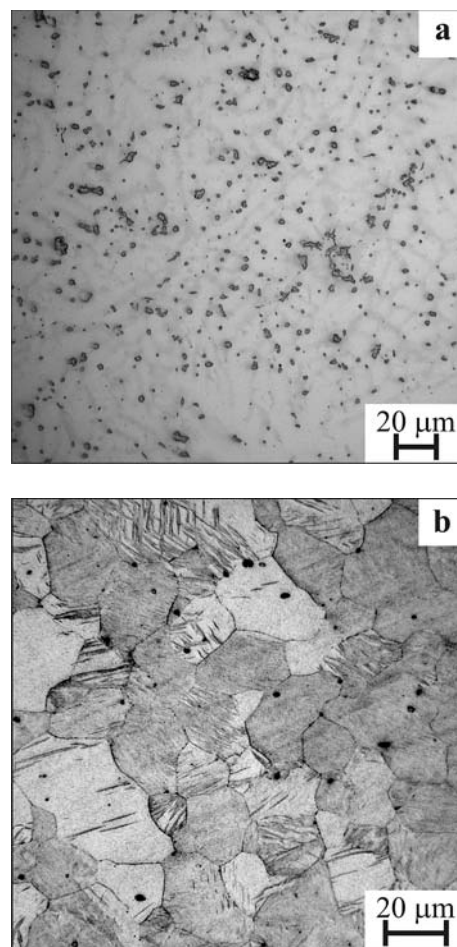


Fig. 2. Microstructure of Mg-4Zn alloys in the as-cast (a) and extruded (b) states. (The horizontal direction of figures of extruded material represents the extrusion direction.)

above 1 mm in size (Fig. 1a). The extrusion process leads to significant grain refining (Fig. 1b) and the average grain size reduces to approximately 25 μm. Grains are recrystallized due to a relatively high extrusion temperature.

If the magnesium is alloyed with 4 wt.% of zinc, the as-cast microstructure is composed of primary dendrites of  $\alpha$ -Mg (light) and interdendritic regions are occupied by secondary phase (black) which is documented in Fig. 2a. Based on the Mg-Zn phase diagram in combination with XRD (Fig. 3a) and EDS (Fig. 4) analyses the secondary phase is determined to be MgZn. Simultaneously to previous case (Fig. 1b), the hot extrusion causes refining of the as-cast structure of the Mg-4Zn alloy (Fig. 2b). The extruded structure is characterized by new dynamically recrystallized grains with the average size of about 20 μm. Moreover, the secondary phase is successfully dissolved during the heat treatment at 340 °C for 24 h applied before extrusion.

Additional alloying of the Mg-4Zn alloys with 0.4 wt.% of calcium leads to an increase of the volume fraction of the secondary phase (Fig. 5a). In the ternary Mg-4Zn-0.4Ca alloy the secondary phase is  $\text{Ca}_2\text{Mg}_6\text{Zn}_3$  as determined by XRD (Fig. 3b) and EDS (Fig. 6). The lattice parameters of  $\text{Ca}_2\text{Mg}_6\text{Zn}_3$  were also determined via X-ray analysis to be  $c = 10.065 \text{ \AA}$ ,  $a = 9.58 \text{ \AA}$ . This is in accordance with the results of Zhang [20]. As it is well documented in Fig. 5b, the extruded Mg-4Zn-0.4Ca alloy exhibits homogeneous equiaxed grained structure with an average grain size close to 6 μm. The above mentioned secondary  $\text{Ca}_2\text{Mg}_6\text{Zn}_3$  phase is not dissolved during heat treatment at 340 °C carried out before the extrusion process. But it is fragmented and aligned parallel to the extrusion direction. In addition, detailed EDS analysis confirms that a small amount of zinc (approximately 3 wt.%; Fig. 6) remains dissolved in the  $\alpha$ -Mg matrix, whereas the concentration of Ca in the  $\alpha$ -Mg phase is negligible (Fig. 5c). All Ca is concentrated in the

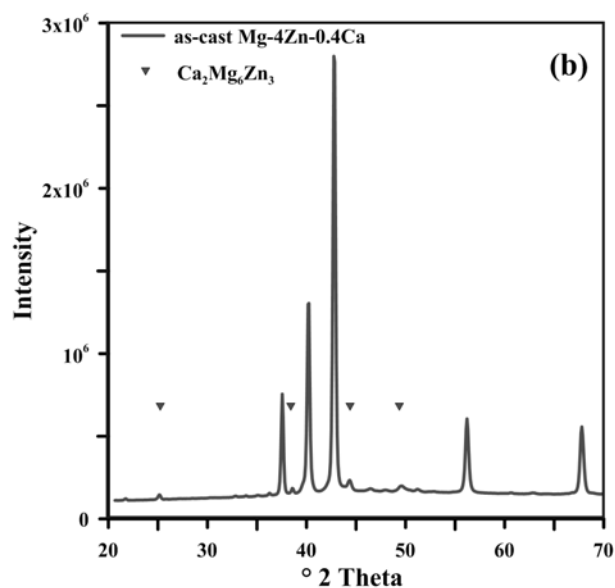
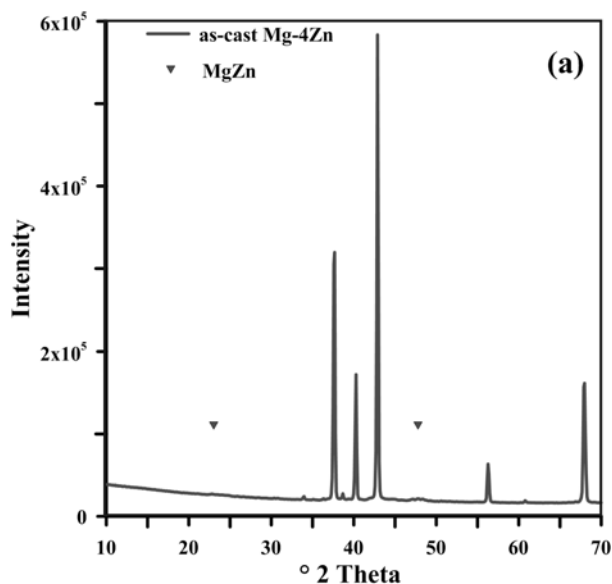


Fig. 3. The X-ray diffraction pattern of as-cast Mg-4Zn (a) and as-cast Mg-4Zn-0.4Ca (b).

$\text{Ca}_2\text{Mg}_6\text{Zn}_3$  secondary phase. This phase effectively blocks the grain growth during hot extrusion.

### 3.2. Mechanical properties

The effects of alloying with zinc and calcium and extrusion process on mechanical properties of magnesium were verified via Vickers hardness measurements as well as compressive and tensile tests. The obtained values of individual mechanical characteristics are summarized in Figs. 7–9. The achieved mechanical properties are discussed with respect to possible dominating strengthening mechanisms, which can be: (i) solid solution strengthening, (ii) secondary phase

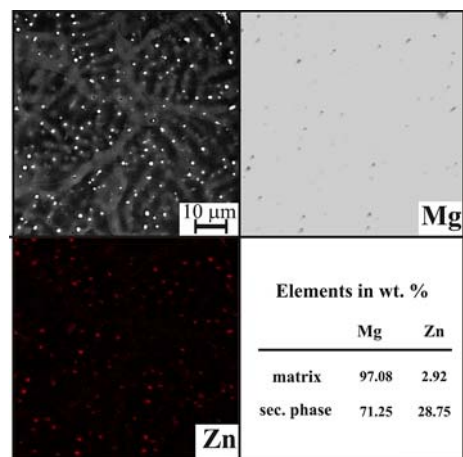


Fig. 4. The X-ray elements distribution map with the results of EDS analyses of the secondary phase and matrix in the as-cast Mg-4Zn alloy.

strengthening or (iii) Hall-Petch (H-P) strengthening. In addition, the effect of texture was verified.

Figure 7 shows that the hardness of magnesium increases due to alloying with Zn and Ca. As shown before, both elements lead to the formation of hard secondary phases (Fig. 2a, Fig. 5a, respectively). In addition, zinc may also contribute to solid solution hardening. Additional increasing of hardness via the process of extrusion is relatively small in the case of pure magnesium and the binary Mg-4Zn alloy. The effect of extrusion on hardness is the most pronounced for the ternary Mg-4Zn-0.4Ca alloy. The main reasons are: (i) presence of the secondary phase and (ii) the most effective grain refining (Fig. 5b).

The room temperature compressive mechanical properties of the investigated alloys are shown in Fig. 8. The compressive yield strength (CYS) follows a similar trend as hardness, i.e., it increases due to additions of zinc and calcium in magnesium in the as-cast states. In contrast to the previous case, the extrusion resulted in increasing of CYS only in the case of pure magnesium. It is caused most likely by refining of the as-cast structure (H-P mechanism; Fig. 1b). A small decrease of CYS for the binary Mg-4Zn alloy due to extrusion can be caused by dissolution of the secondary phase before the extrusion process (Fig. 2b). It can be assumed that dissolution of the interdendritic intermetallic phases (Fig. 2) makes compressive plastic strain easier. Additional explanation can be that small zinc atoms introduced into the hexagonal magnesium lattice may result in decreasing of the critical resolve shear stress for activation of the non-basal slip system, which results in improved plasticity of the Mg-based alloys [21, 22]. Surprisingly, a change of the CYS value in the case of the ternary Mg-4Zn-0.4Ca alloy is negligible. It can be explained by the strong effect of the secondary phase (Fig. 5). In contrast to the

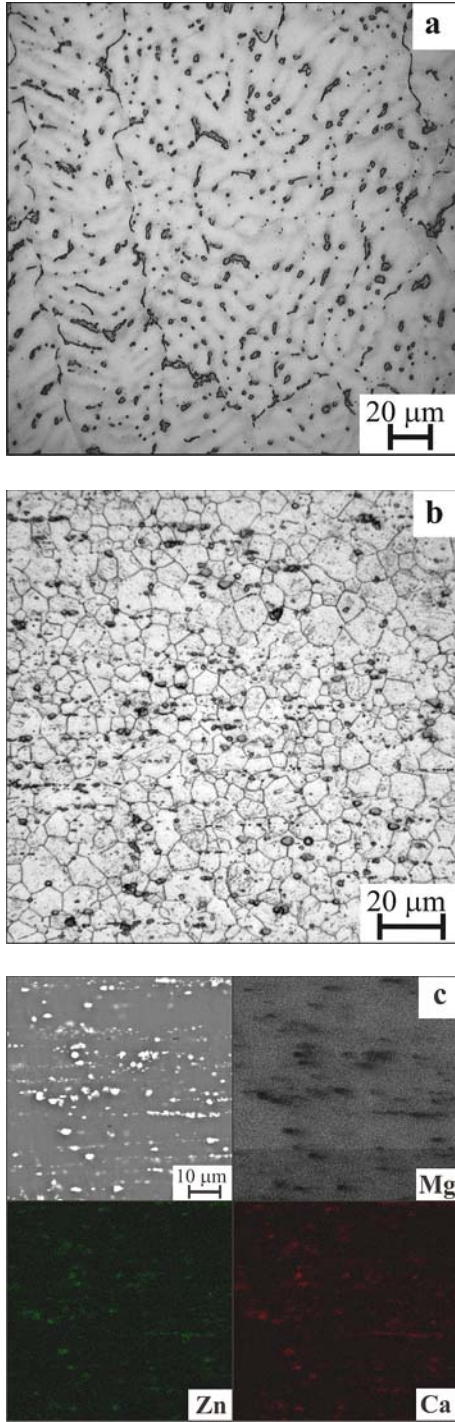


Fig. 5. Microstructure of Mg-4Zn-0.4Ca in the as-cast (a) and extruded (b) states with an X-ray elements distribution map (c). (The horizontal direction of figures of extruded material represents the extrusion direction.)

CYS, the values of the ultimate compressive strength (UCS) are significantly improved by both the alloying elements and the process of extrusion (Fig. 8b). In the case of the ternary alloy treated by extrusion the UCS achieves 440 MPa. These results confirm the assump-

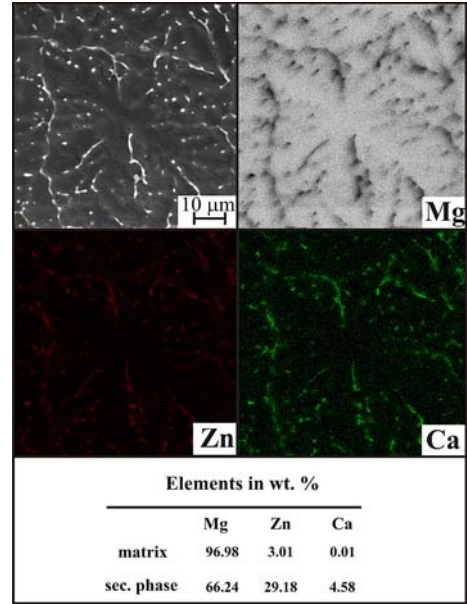


Fig. 6. The X-ray elements distribution map with the results of EDS analyses of the secondary phase and matrix in the as-cast Mg-4Zn-0.4Ca alloy.

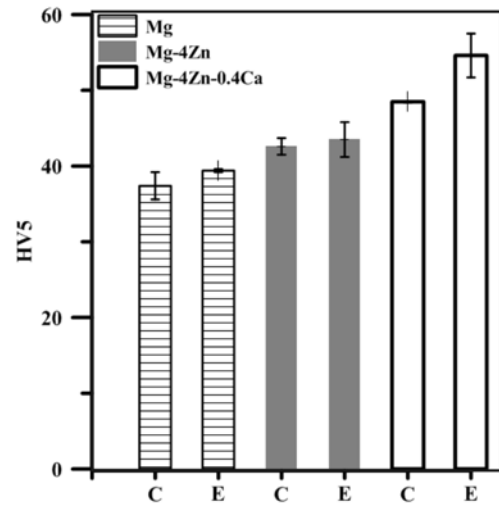


Fig. 7. Hardness (HV5) of the investigated materials in the as-cast (C) and extruded (E) states.

tion that addition of Ca to Mg-Zn alloys may improve hardening and strengthening effects.

The tensile properties measured at RT are given in Fig. 9. The average tensile yield strength (TYS) and ultimate tensile strength (UTS) for as-cast magnesium are as low as 33 and 96 MPa, respectively. However, with the addition of 4 wt.% Zn, the TYSS and UTS are more than twofold increased to 110 and 233 MPa, respectively. The additional alloying with calcium does not lead to further increasing of these characteristics. The improving TYSS and UTS of the as-cast states of

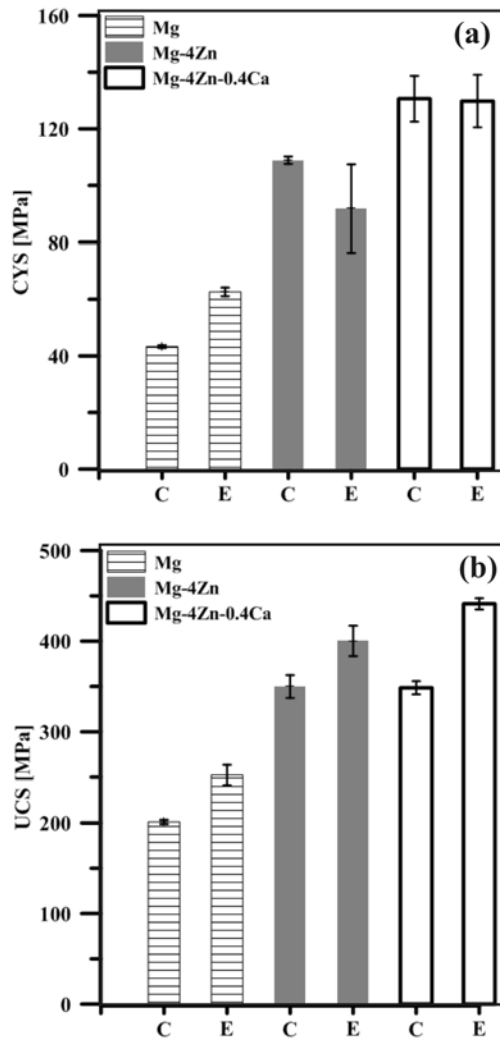


Fig. 8. Compressive yield strength (CYS) (a) and ultimate compressive strength (UCS) (b) of the investigated materials in the as-cast (C) and extruded (E) states.

both magnesium alloys could be attributed preferentially to the presence of the secondary phases (Figs. 2a, 3, 5a).

However, applying of extrusion results in further twofold increase of the TYS (Fig. 9a). Such changes could be ascribed to two effects, namely decreasing the grain size (Figs. 1b, 2b, 5b) and changing the texture (Fig. 10). Usually, magnesium alloys tend to develop sharp prismatic texture during extrusion that aligns basal planes of deformed grains parallel to the extrusion direction ED [23]. Such texture is strong for activation of basal slip which mainly operates during deformation at RT [24]. To achieve appropriate orientation of basal planes and thus plastically deform Mg and its alloys, higher stress has to be imposed, thus the values of TYS are increased. Comparably, the value of UTS of pure magnesium is almost twice increased as a result of the extrusion process (Fig. 9b),

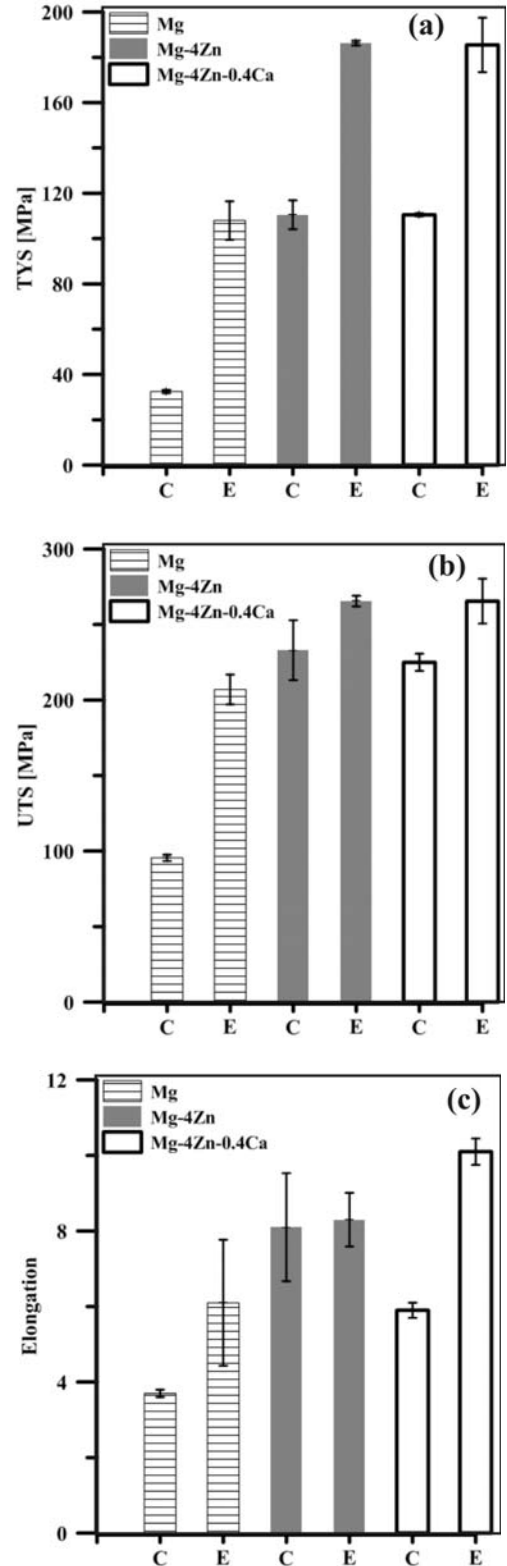


Fig. 9. Tensile mechanical properties of the as-cast (C) and extruded (E) investigated materials: (a) tensile yield strength (TYS), (b) ultimate tensile strength (UTS) and (c) elongation.

and it could be ascribed to the effect of decreasing the average grain size and H-P strengthening. Although

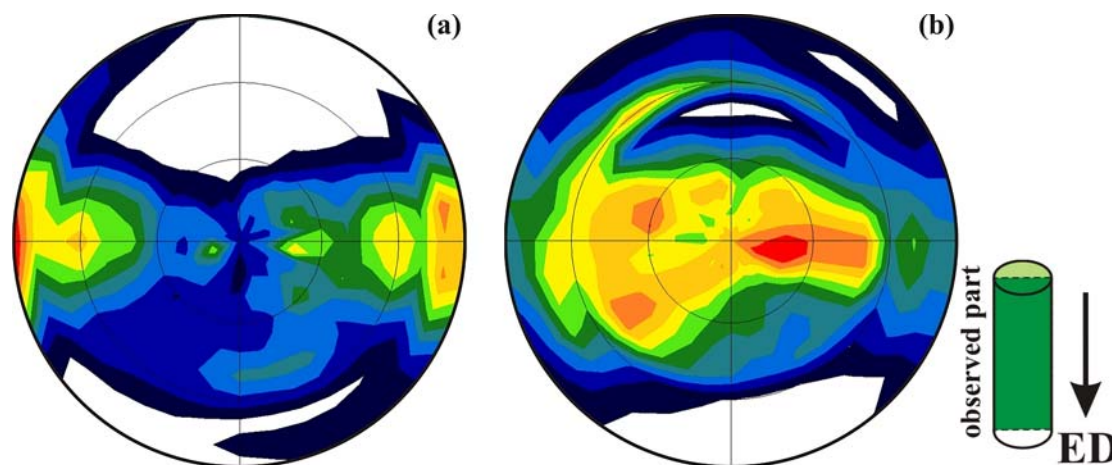


Fig. 10. The (0002) pole figures of Mg-4Zn (a) and Mg-4Zn-0.4Ca (b) alloys processed by extrusion.

the UTS of the Mg-4Zn and Mg-4Zn-0.4Ca alloys are also improved by extrusion and possess values higher than 260 MPa, these changes are not so pronounced as in the case of the TYS.

The textures of extruded Mg-4Zn and Mg-4Zn-0.4Ca were additionally verified by X-ray measurement and results are given in Fig. 10. It can be seen that the  $c$ -axis of hcp crystal is predominantly aligned perpendicular to the extrusion direction (ED) in both investigated alloys as was previously suggested. Nevertheless, the addition of calcium evoked changes of the maximum of  $c$ -axis orientation in the position and intensity. In the ternary alloy, the  $c$ -axis inclined closer to the centre of the pole figures and its intensity is decreased. As the extrusion texture may be changed under the operating recrystallization [25], the secondary  $\text{Ca}_2\text{Mg}_6\text{Zn}_3$  phase particles in the ternary alloy seem to play more important role during texture evolution. The presence of  $\text{Ca}_2\text{Mg}_6\text{Zn}_3$  particles may support the formation of recrystallized grains via particle-stimulated nucleation (PSN) mechanism, which may result in different orientation of the grains in the recrystallized microstructure [26]. The possible operating of PSN during deformation of Mg-Zn-Ca alloy was suggested in [27].

It is possible to interpret this situation by nucleation of new grains with random orientation in the case of ternary alloy, however, it can be changed during the deformation process. Thus the final extrusion texture with the perpendicularly oriented  $c$ -axis to ED is remained, but the intensities of the orientation position are decreased. Simultaneous effect was observed in AZ31 alloy doped by Ca and rare earth elements [28]. In addition, high orientation mismatch was also ascribed to activation of PSN mechanism during extrusion of the AZ31 alloys with addition of 0.4–0.8 wt.% Sr carried out at 350 °C [29]. In spite of that, the TYS remains comparable as in the case of the binary alloy with sharper texture. This can be explained by

the effect of the secondary phase and smaller grain size, which both can make the tensile deformation more difficult, thus contribute to strengthening of the ternary alloy.

The results in Fig. 9c show how the elongation is influenced by alloying with zinc, calcium and by extrusion. It can be seen that the elongation of extruded alloys achieves higher values as compared to the as-cast state, in which zinc has the most positive effect on plasticity. However, application of hot extrusion has only small effect on the increasing elongation of Mg-4Zn in spite of that extruded binary alloy is dominated by the plastic  $\alpha$ -Mg solid solution. This should be ascribed to an inappropriate modification of the texture (Fig. 10a) which does not allow the alloys to be suitably plastically deformed as activation of the slip systems is difficult and thus, the tensile stress cannot be accommodated by them. Thus the imposed stress is accumulated and as a result, cracks can nucleate more easily. This limits ductility in the binary alloy. On the other hand, the best elongation of 10 % is achieved in the case of the extruded Mg-4Zn-0.4Ca ternary alloy. This could be preferentially attributed to the considerable grain refinement caused by extrusion (Fig. 5b). In addition, the fragmentation and better distribution of secondary phase may also contribute to increasing elongation by partial carrying the applied strain and local plastic deformation, which may take place in the vicinity of particles of these secondary  $\text{Ca}_2\text{Mg}_6\text{Zn}_3$  phases.

The following Figs. 11–13 show fracture surfaces of magnesium and its alloys after tensile tests. A combination of inter- and trans-crystalline failures can be observed for the as-cast pure Mg (Fig. 11a). In the case of extruded magnesium (Fig. 11b), plastic deformation can be locally observed, which is in accordance with the slightly higher elongation measured in comparison with the as-cast state of magnesium (Fig. 9c).

In as-cast Mg-4Zn alloy (Fig. 12a, in detailed

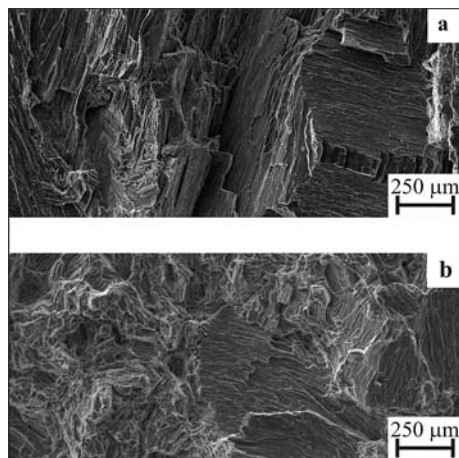


Fig. 11. Fracture surfaces of the as-cast (a) and extruded (b) magnesium after tensile tests.

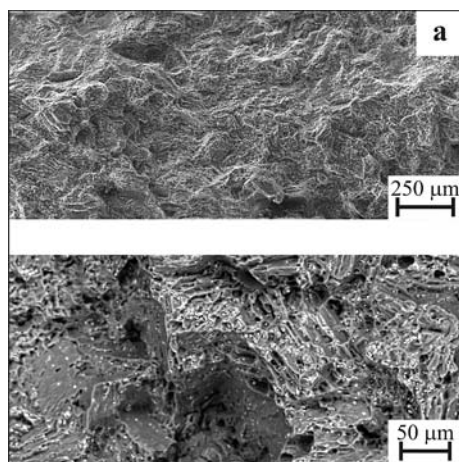


Fig. 12. Fracture surfaces of the as-cast (a) and extruded (b) Mg-4Zn alloy after tensile tests.

view), fracture cracks grow across the dendrites and along dendrite boundaries, which are occupied by

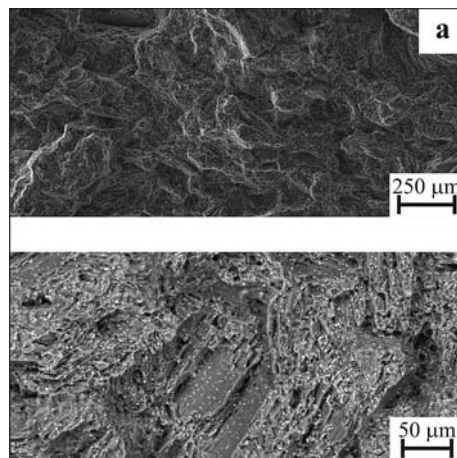


Fig. 13. Fracture surfaces of the as-cast (a) and extruded (b) Mg-4Zn-0.4Ca alloy after tensile tests.

the secondary phase acting as stress concentrators. Particles of this phase are clearly visible in Fig. 12a as fine light spots in the detailed image. During loading of the extruded binary Mg-4Zn alloy the fracture is trans-crystalline (Fig. 12b) and a more detailed view indicates the occurrence of local plastic deformation during fracture.

The fracture surface of as-cast Mg-4Zn-0.4Ca alloy shown in Fig. 13a is similar to that of the binary one. But, the fracture surface of the extruded Mg-4Zn-0.4Ca (Fig. 13b) alloy exhibits more places with the local plastic deformation. The presence of small and deep dimples surrounding hard  $\text{Ca}_2\text{Mg}_6\text{Zn}_3$  particles is the evidence of the plastic deformation at such places which contribute to achieving the highest elongation in the case of the ternary alloy (Fig. 9c). In addition, the observed refining of the fracture surface of the extruded Mg-4Zn-0.4Ca alloy in comparison with the other alloys can be ascribed to the most refining effect of the extrusion process (Fig. 5b).

In summary, it is shown that in the case of as-cast state, the dominant strengthening effect is via second-



ary phase. In extruded samples, final mechanical characteristics result from combination of all strengthening mechanisms, namely: (i) solid solution strengthening, (ii) secondary phase strengthening and (iii) Hall-Petch (H-P) strengthening, which are the most pronounced in the ternary alloy. Additionally, the extruded ternary Mg-4Zn-0.4Ca alloy exhibits values of UTS and TYS comparable with the widely investigated AZ31 alloy processed by more complicated ECAP technique [30].

#### 4. Conclusions

The achieved results led to the following conclusions:

1. Addition of zinc and calcium led to dendritic microsegregation and formation of the secondary phase during casting. The presence of the secondary phase successfully improved all tested mechanical properties.

2. Applying of extrusion further increased the mechanical characteristics of magnesium and its alloys due to the refining their structure. This effect was the most pronounced in the case of TYS values.

3. The addition of small amount of calcium contributed to improvement of most of tested mechanical properties, to weaken the extrusion texture and to decreasing of the average grain size close to 6  $\mu\text{m}$ .

The present work showed that alloying of magnesium with low-cost elements in combination with the widely used extrusion process can produce lightweight materials with a very good combination of mechanical properties. These materials will be further tested for creep and corrosion in the following research.

#### Acknowledgements

The authors would like to thank the Czech Science Foundation (project no. P108/12/G043) for financial support.

#### References

- [1] Hsiang, S. H., Lin, Y. W.: *J. Mater. Process. Technol.*, 192–193, 2007, p. 292. [doi:10.1016/j.jmatprotec.2007.04.063](https://doi.org/10.1016/j.jmatprotec.2007.04.063)
- [2] Hsiang, S.-H., Kuo, J.-L.: *J. Mater. Process. Technol.*, 140, 2003, p. 6. [doi:10.1016/S0924-0136\(03\)00693-9](https://doi.org/10.1016/S0924-0136(03)00693-9)
- [3] Hono, K., Mendis, C. L., Sasaki, T. T., Oh-ishi, K.: *Scripta Mater.*, 63, 2010, p. 710. [doi:10.1016/j.scriptamat.2010.01.038](https://doi.org/10.1016/j.scriptamat.2010.01.038)
- [4] Ma, A., Jiang, J., Saito, N., Shigematsu, I., Yuan, Y., Yang, D., Nishida, Y.: *Mater. Sci. Eng. A*, 513–514, 2009, p. 122. [doi:10.1016/j.msea.2009.01.040](https://doi.org/10.1016/j.msea.2009.01.040)
- [5] Hamu, G. B., Eliezer, D., Wagner, L.: *J. Alloys Compd.*, 468, 2009, p. 222. [doi:10.1016/j.jallcom.2008.01.084](https://doi.org/10.1016/j.jallcom.2008.01.084)
- [6] Suwas, S., Gottstein, G., Kumar, R.: *Mat. Sci. Eng. A*, 471, 2007, p. 1. [doi:10.1016/j.msea.2007.05.030](https://doi.org/10.1016/j.msea.2007.05.030)
- [7] Biswas, S., Suwas, S., Sikand, R., Gupta, A. K.: *Mat. Sci. Eng. A*, 528, 2011, p. 3722. [doi:10.1016/j.msea.2011.01.021](https://doi.org/10.1016/j.msea.2011.01.021)
- [8] Witte, F., Hort, N., Vogt, C., Cohen, S., Kainer, K. U., Willumeit, R., Feyerabend, F.: *Curr. Opin. Solid State Mater. Sci.*, 12, 2008, p. 63. [doi:10.1016/j.cossms.2009.04.001](https://doi.org/10.1016/j.cossms.2009.04.001)
- [9] Smola, B., Stulíková, I., Pelcová, J., Mordike, B. L.: *J. Alloys Compd.*, 378, 2004, p. 196. [doi:10.1016/j.jallcom.2003.10.099](https://doi.org/10.1016/j.jallcom.2003.10.099)
- [10] Massalski, T. B., Murray, J. L., Bennett, L. H., Baker, H.: *Binary Alloy Phase Diagrams*. Metals Park, American Society for Metals 1986.
- [11] Hradilová, M., Vojtěch, D., Kubásek, J., Čapek, J., Vlach, M.: *Mat. Sci. Eng. A*, 586, 2013, p. 284. [doi:10.1016/j.msea.2013.08.008](https://doi.org/10.1016/j.msea.2013.08.008)
- [12] Guan, R., Cipriano, A. F., Zhao, Z., Lock, J., Tie, D., Zhao, T., Cui, T., Liu, H.: *Mater. Sci. Eng. C*, 581, 2013, p. 31. [doi:10.1016/j.msea.2013.05.055](https://doi.org/10.1016/j.msea.2013.05.055)
- [13] Yang, M., Cheng, L., Pan, F.: *J. Mater. Sci.*, 44, 2009, p. 4577. [doi:10.1007/s10853-009-3696-0](https://doi.org/10.1007/s10853-009-3696-0)
- [14] Rosalbino, F., Negri, S., Saccone, A., Angelini, E., Delfino, S.: *J. Mater. Sci.-Mater. Med.*, 21, 2010, p. 1091. [doi:10.1007/s10856-009-3956-1](https://doi.org/10.1007/s10856-009-3956-1)
- [15] Gao, X., Zhu, S. M., Muddle, B. C., Nie, J. F.: *Scripta Mater.*, 53, 2005, p. 1321. [doi:10.1016/j.scriptamat.2005.08.035](https://doi.org/10.1016/j.scriptamat.2005.08.035)
- [16] Zhang, S., Zhang, X., Zhao, C., Li, J., Song, Y., Xie, C., Tao, Y., Zhang, Y., He, Y., Jiang, Y., Bian, Y.: *Acta Biomater.*, 6, 2010, p. 626. [doi:10.1016/j.actbio.2009.06.028](https://doi.org/10.1016/j.actbio.2009.06.028)
- [17] Boehlert, C. J., Knittel, K.: *Mater. Sci. Eng. A*, 417, 2006, p. 315. [doi:10.1016/j.msea.2005.11.006](https://doi.org/10.1016/j.msea.2005.11.006)
- [18] Wang, Y., Wu, G., Liu, W., Pang, S., Zhang, Y., Ding, W.: *Mater. Sci. Eng. A*, 594, 2014, p. 52. [doi:10.1016/j.msea.2013.11.040](https://doi.org/10.1016/j.msea.2013.11.040)
- [19] Cai, S., Lei, T., Li, N., Feng, F.: *Mater. Sci. Eng. C*, 32, 2012, p. 2570. [doi:10.1016/j.msec.2012.07.042](https://doi.org/10.1016/j.msec.2012.07.042)
- [20] Zhang, Y. N., Kevorkov, D., Li, J., Essadiqi, E., Medraj, M.: *Intermetallics*, 18, 2010, p. 2404. [doi:10.1016/j.intermet.2010.08.033](https://doi.org/10.1016/j.intermet.2010.08.033)
- [21] Akhtar, A., Teghtsoonian, E.: *Acta Metall.*, 17, 1969, p. 1339. [doi:10.1016/0001-6160\(69\)90151-5](https://doi.org/10.1016/0001-6160(69)90151-5)
- [22] Akhtar, A., Teghtsoonian, E.: *Acta Metall.*, 17, 1969, p. 1351. [doi:10.1016/0001-6160\(69\)90152-7](https://doi.org/10.1016/0001-6160(69)90152-7)
- [23] Al-Samman, T.: *Mater. Sci. Eng. A*, 560, 2013, p. 561. [doi:10.1016/j.msea.2012.09.102](https://doi.org/10.1016/j.msea.2012.09.102)
- [24] Avedesian, M. M., Baker, H.: *Magnesium and Magnesium Alloys*. Materials Park, ASM International 1999.
- [25] Bohlen, J., Yi, S. B., Swiostek, J., Letzig, D., Brokmeier, H. G., Kainer, K. U.: *Scripta Mater.*, 53, 2005, p. 259. [doi:10.1016/j.scriptamat.2005.03.036](https://doi.org/10.1016/j.scriptamat.2005.03.036)
- [26] Humphreys, F. J., Hatherly, M.: *Recrystallization and Related Annealing Phenomena*. Oxford, Elsevier 2004.
- [27] Hradilová, M., Montheillet, F., Frazekiewicz, A., Desrayaud, C., Lejček, P.: *Mater. Sci. Eng. A*, 580, 2013, p. 217. [doi:10.1016/j.msea.2013.05.054](https://doi.org/10.1016/j.msea.2013.05.054)

- [28] Laser, T., Hartig, C., Nürnberg, M. R., Letzig, D., Bormann, R.: *Acta Mater.*, 56, 2008, p. 2791.  
[doi:10.1016/j.actamat.2008.02.010](https://doi.org/10.1016/j.actamat.2008.02.010)
- [29] Sadeghi, A., Hoseini, M., Pegguleryuz, M.: *Mater. Sci. Eng. A*, 528, 2011, p. 3096.  
[doi:10.1016/j.msea.2010.12.091](https://doi.org/10.1016/j.msea.2010.12.091)
- [30] Xia, K., Wang, J. T., Wu, X., Chen, G., Gurvan, M.: *Mater. Sci. Eng. A*, 410–411, 2005, p. 324.  
[doi:10.1016/j.msea.2005.08.123](https://doi.org/10.1016/j.msea.2005.08.123)